Liquid Crystals
Publication details, including instructions for authors and subscription information:
http://www.informaworld.com/smpp/title~content=t713926090

New banana-shaped mesogens with bromine-substituted central core

H. Dehne; M. Pötter; S. Sokolowski; W. Weissflog; S. Diele; G. Pelzl; I. Wirth; H. Kresse; H. Schmalfuss; S. Grande

Online publication date: 06 August 2010

To cite this Article Dehne, H. , Pötter, M. , Sokolowski, S. , Weissflog, W. , Diele, S. , Pelzl, G. , Wirth, I. , Kresse, H. , Schmalfuss, H. and Grande, S.(2001) 'New banana-shaped mesogens with bromine-substituted central core', Liquid Crystals, 28: 8, 1269 — 1277
To link to this Article: DOI: 10.1080/02678290110047904
URL: http://dx.doi.org/10.1080/02678290110047904

LIQUID CRYSTALS, 2001, VOL. 28, NO. 8, 1269–1277

New banana-shaped mesogens with bromine-substituted central core

H. DEHNE, M. PÖTTER, S. SOKOLOWSKI

Fachbereich Chemie, Universität Rostock, Buchbinderstr. 9, D-18055 Rostock, Germany

W. WEISSFLOG*, S. DIELE, G. PELZL, I. WIRTH, H. KRESSE, H. SCHMALFUSS

Institut für Physikalische Chemie, Martin-Luther-Universität Halle-Wittenberg, Mühlpforte 1, D-06108 Halle, Germany

and S. GRANDE

Fakultät für Physik und Geowissenschaften, Universität Leipzig, Linnéstr. 5, D-04103 Leipzig, Germany

(*Received 9 November 2000; accepted 8 January 2001*)

Banana-shaped five-ring mesogens derived from either isophthalic acid or 4-bromoisophthalic acid have been synthesized. It is shown that the melting and clearing points of the bromine-substituted compounds are markedly decreased in comparison with the analogous unsubstituted compounds. On the basis of X-ray diffraction studies and NMR measurements, as well as dielectric and electro-optical investigations, the mesophase of these compounds could be identified as a B_2 phase.

1. Introduction

Bent mesogens represent a topical field in current liquid crystal research. Due to their shape the molecules are able to create a polar ordering within the smectic layers [1]. Together with a tilt of the molecular long axis, the symmetry breaking can lead to chiral discrimination [2]. Therefore, some B-phases (B_2, B_5, B_7) exhibit a ferro-/antiferro-electric switching behaviour although the single molecules are non-chiral [3]. Most of the banana-shaped liquid crystal molecules reported in the literature up to now contain a 1,3-phenylene fragment to create a bending angle of about 120° [3–5]. Many compounds are derived from resorcinol, which serves as the central unit [5, 6]. In contrast, esters of isophthalic acid have been reported only by Nguyen *et al.* [7]. They described nematic and smectic phases for bis[4-(4-alkoxybenzoylthio)phenyl] isophthalates. The introduction of fluorine in lateral positions of the outer rings of these molecules changed the polymorphism markedly. Four different smectic phases without in-plane order were detected, but the assignment of the phases has not been completed up to now.

*Author for correspondence; e-mail: weissflog@chemie.uni-halle.de

The influence of small lateral substituents on the mesophase behaviour of banana-shaped compounds is a further aspect of interest that has been studied by several research groups. The different positions of substitution must be distinguished. The outer rings can most probably be substituted without loss of the liquid crystalline properties [7–9]. The disturbing effect seems to be very large if the rings situated more inside the molecules are laterally substituted [10]. Many investigations have been made to study the influence of halogen atoms or small groups positioned at the central 1,3-phenylene ring, especially for derivatives of resorcinol. Even small substituents in the 5-position at the top of five-ring molecules, except for fluorine, prevent the formation of mesophases [6]. Small groups like methyl or nitro can be introduced into position 2, that is in the obtuse angle of the bent mesogen, and can result in interesting phases such as B_5 and B_7, respectively [3, 11, 12]. Introduction of substituents is possible in the 4-position, for example, liquid crystalline esters not only of 4-chloro- and 4-cyano-resorcinol, but also of 4,6-dichlororesorcinol, have been reported [3, 13–16]. It is important to recognize that substituents which are attached at the central phenylene ring can change the conformation of the whole molecule. While the bending angle of

Liquid Crystals ISSN 0267-8292 print/ISSN 1366-5855 online © 2001 Taylor & Francis Ltd
http://www.tandf.co.uk/journals
DOI: 10.1080/02678290110047904

1,3-phenylene bis[4-(4-*n*-octyloxyphenyliminomethyl)-benzoate] is about 120°, the angle is increased up to 131° and to about 165°, respectively, for the related derivatives of 4-chloro- and 4,6-dichloro-resorcinol [3, 16].

In this paper, esters of isophthalic acid are used to study the influence of the direction of orientation of the carboxylate groups at the central benzene ring. Furthermore, starting with 4-bromoisophthalic acid, the influence of this halogen atom on the mesophase behaviour, the molecular conformation and selected physical properties are investigated by different methods, e.g. X-ray, NMR studies, and dielectric and electro-optical measurements.

2. Materials

The banana-shaped molecules studied can be represented by the following general formula:

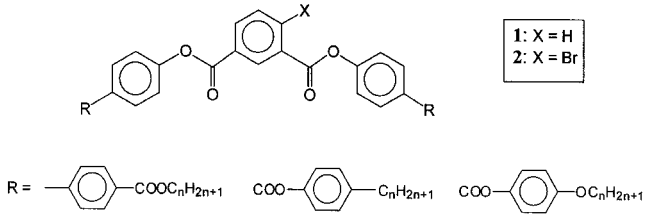

The isophthalic acid diesters **1** and **2** were prepared by reaction of isophthaloyl chloride or 4-bromoisophthaloyl chloride in pyridine with the corresponding phenols, i.e. alkyl esters of 4-hydroxybiphenyl-4′-carboxylic acid and 4-(4-alkyl- or 4-alkoxy-phenoxycarbonyl)phenols. The reaction mixture was stirred at room temperature for 8 h and worked up in the usual way. The purification of the raw materials was achieved by recrystallization from ethanol/toluene or ethanol/DMF. The yields were greater than 80% after the first recrystallization.

The melting behaviour of the isophthalic acid diesters is summarized in table 1, and that of the 4-bromo-isophthalic diesters in table 2 [17].

The clearing points of the isophthalic acid diesters **1** are much higher than those of comparable derivatives of resorcinol. For example, the inversion of all carboxylate groups of compound **1e**, which exhibits a mesophase up to 193°C, results in the corresponding resorcinol derivative having a clearing point of 121°C [3]. However, in most cases the isophthalic acid compounds **1** exhibit high melting points, and therefore only for one homologue **1h** could an enantiotropic mesophase be detected.

Starting with 4-bromoisophthalic acid, the melting as well as the clearing points of the resulting esters **2** are decreased. Because the melting temperatures are reduced more, substances with enantiotropic mesophases exist, and these are suitable for further investigations. By introduction of the bromine atom in the central benzene unit of the five-ring isophthalic acid diesters, the mesophase stability is reduced by about 25–35 K, as seen by comparison of the clearing temperatures of corresponding bromine-substituted and unbrominated compounds.

Table 1. Phase transition temperatures (°C) of compounds **1** (X = H).

Compound	R_1	Cr		B_2		I
1a	COO-C$_6$H$_4$-C$_5$H$_{11}$	•	200	—		•
1b	COO-C$_6$H$_4$-C$_7$H$_{15}$	•	188	—		•
1c	COO-C$_6$H$_4$-C$_9$H$_{19}$	•	184	(•[a]	178)	•
1d	COO-C$_6$H$_4$-OC$_6$H$_{13}$	•	210	—		•
1e	COO-C$_6$H$_4$-OC$_8$H$_{17}$	•	205	(•[a]	193)	•
1f	COO-C$_6$H$_4$-OC$_{10}$H$_{21}$	•	199	(•[a]	194)	•
1g	C$_6$H$_4$-COOC$_2$H$_5$	•	234	—		•
1h	C$_6$H$_4$-COOC$_3$H$_7$	•	181	•	204	•
1i	C$_6$H$_4$-COOC$_4$H$_9$	•	196	(•	188)	•

[a] Phase assignment based on the optical texture only.

3. Experimental

The thermal behaviour of the compounds was investigated using a Perkin Elmer DSC 7 differential scanning calorimeter. The microscopic textures and the field-induced changes of the textures were examined using a polarising optical microscope (Leitz Orthoplan) equipped with a Linkam THM 600/S hot stage.

X-ray investigations on non-oriented samples were carried out using a Guinier-film-camera and a Guinier-Goniometer (Huber Diffraktionstechnik GmbH). Oriented samples were obtained by annealing a drop of liquid crystal placed on a glass plate. In this case the beam was incident nearly parallel to the glass plate. X-ray patterns were recorded with a 2D-detector (HI-Star, Siemens AG). Because of the special sample preparation only the scattering intensity of the upper half of the reciprocal space could be recorded.

NMR measurements were made using a Bruker MSL 500 spectrometer at a field of 11.7 T. The temperature of the 5 mm sample tubes was regulated by a Bruker BST-100 temperature controller. Simple pulse excitations and cross-polarization experiments with continuous or

Table 2. Phase transition temperatures (°C) of the compounds **2** (X = Br).

Compound	R_1	Cr		B_2		I
2a	COO-◯-C_5H_{11}	•	133	(•	129)	•
2b	COO-◯-C_9H_{19}	•	127	•	145	•
2c	COO-◯-OC_5H_{11}	•	136	•	164	•
2d	COO-◯-OC_6H_{13}	•	135	•	164	•
2e	COO-◯-OC_7H_{15}	•	138	•	164	•
2f	COO-◯-OC_8H_{17}	•	132	•	166	•
2g	COO-◯-OC_9H_{19}	•	130	•	166	•
2h	COO-◯-$OC_{10}H_{21}$	•	130	•	167	•
2i	-◯-$COOC_2H_5$	•	202	—		•
2j	-◯-$COOC_2H_5$	•	165	(•	147)	•

pulsed ^{1}H decoupling were used for the ^{13}C NMR at 125 MHz. The amplitude of the decoupling field in liquid crystalline phases was as low as possible (0.6–0.8 mT) to avoid heating of the sample.

Dielectric measurements were performed using the HP 4192A and the Solartron Schlumberger SI 1260 impedance analyser. The samples were put in a double plate capacitor ($A = 2\,cm^2$, $d = 0.02\,cm$) which was calibrated with cyclohexane.

Electro-optical investigations were carried out using the usual experimental set-up where the cells are heated on the hot stage of a polarizing microscope and a power supply (Keithley 3910) generates the voltage signals. The triangular wave method was used to investigate the current response of the cells.

4. Experimental results

4.1. *Optical textures*

On cooling the isotropic liquid, the mesophase preferentially forms oval nuclei. They coalesce to a beautiful non-uniform texture which consists of unspecific 'grainy' regions together with fan-like and circular domains, as shown in figures 1 and 2, respectively. These domains frequently show irregular stripes parallel to the smectic

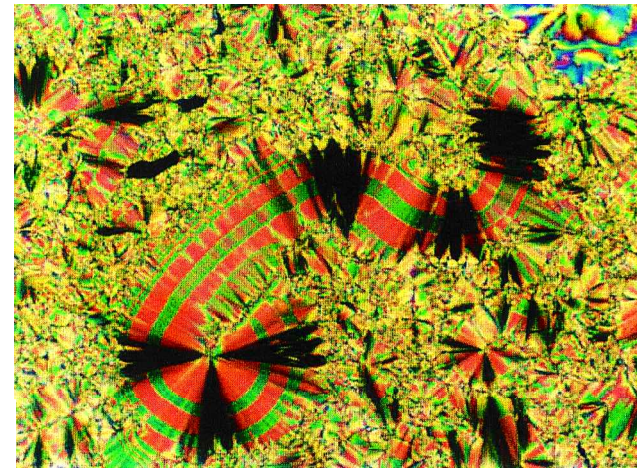

Figure 1. Texture with circular domains of the B_2 phase of compound **2d** (160°C).

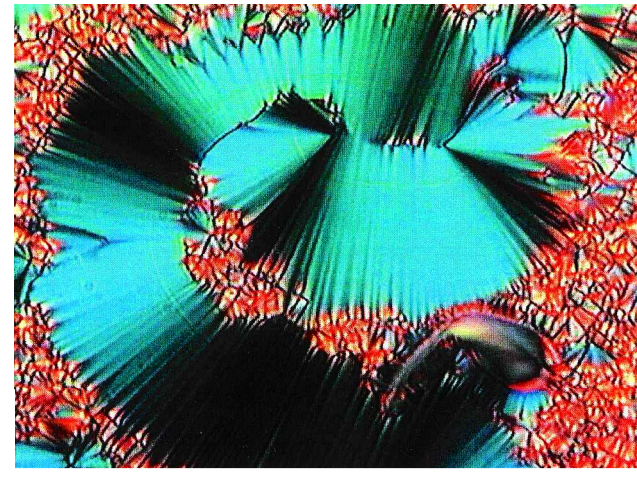

Figure 2. Fan-shaped texture and grainy texture of the B_2 phase of compound **1h** (194°C).

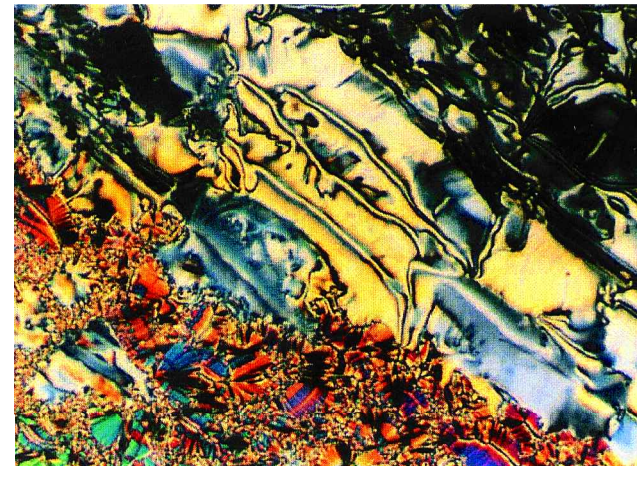

Figure 3. Schlieren texture of the B_2 phase of compound **2d** (160°C).

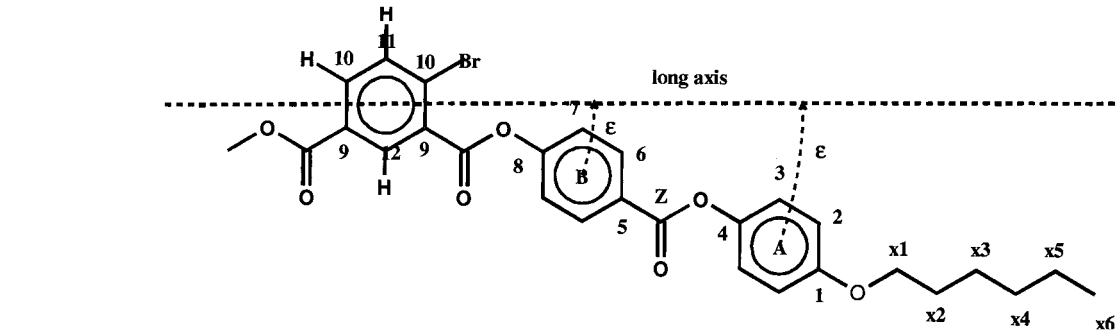

(*a*)

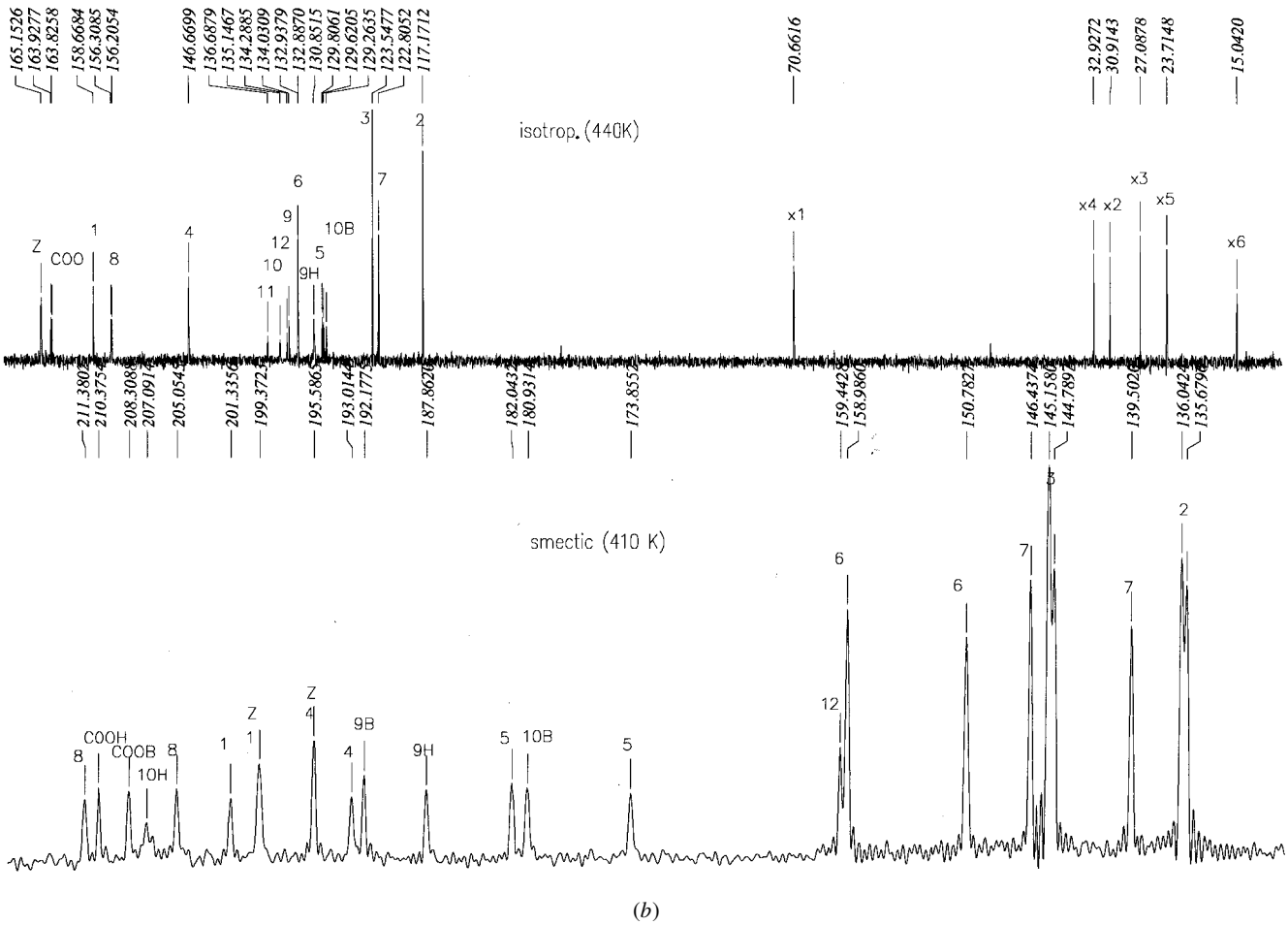

(*b*)

Figure 4. (*a*) Sketch of the molecule and assignment of the atoms and rings of compound **2d**. Also shown is a molecular long axis in a symmetric position. The torsion angles (table 3) refer to a rotation of the segmental planes with respect to the plane of the whole molecules. (*b*) ^{13}C spectrum of compound **2d** at 125 MHz in the isotropic phase at 440 K (upper: pulsed WALTZ-decoupling, 40 scans) and in the smectic phase at 416 K (lower: $\Delta T = 12$ K, CP excitation with WALTZ-decoupling, 80 scans). The isotropic shifts of the aromatic region for compound **2h** agree with the values shown above each spectrum. Small differences in the anisotropic shifts in the liquid crystalline phase change the overlapping of lines.

layers. In the circular domains, the smectic layers are arranged circularly with the result that the layer planes are more or less perpendicular to the substrate. This is indicated by the black extinction cross which coincides with the directions of the crossed polarizers and which does not change on rotating the sample. Depending on the surface conditions schlieren-like textures can also be observed (figure 3).

4.2. *NMR measurements*

NMR measurements were performed on compounds **2d** and **2h**. Figure 4(*b*) displays the ^{13}C spectra for the isotropic and liquid crystalline states. The assignment of the lines was carried out in a similar way to that described for other banana-shaped mesogens [14]. In figure 4(*a*) the molecular structure is sketched and the individual carbon atoms are designated. In addition, the molecular long axis is drawn in a symmetric position. The angle ε corresponds to the angle between the molecular long axis and the *para*-axis of aromatic rings B and A, respectively. From ε the bending angle $\alpha = 180° - 2\varepsilon$ can be determined. The torsion angle φ refers to a rotation of the segmental planes with respect to the plane of the whole molecule.

The central ring is not involved in intramolecular motions and defines the skeleton of the molecule. We use the anisotropic shifts of carbons 9 and 10 to evaluate the order parameter S (neglecting contributions from D). The values shown in figure 5 are high and increase slightly with decreasing temperature.

Using S we can extract the anisotropic shifts for the C^i belonging to the rings and linkage groups of both legs. Their magnitude depends on the time-averaged geometry, that is, on the angle ε and the torsion angle φ (figure 4). We have compared the derived values with those of single rod-like reference molecules which consist of two aromatic rings and of the same linkage groups as the legs of the banana-shaped molecules under discussion. As shown in [11, 14], in this way the angles ε and φ for the segmental rings and the linkage groups can be determined and these are summarized in table 3. It is obvious from the table that similarly to chlorine-substituted banana-shaped molecules, the two legs of the molecules are not completely symmetrically disposed with respect to the molecular long axis, but the difference is not pronounced (1°–2°).

The absolute values of the angles depend on the assumed model, but the values obtained for the rings in the different compounds are more precise. The two molecules have similar geometries. The torsion of the carboxylate groups at the central ring also rotates the dipole moments of these groups by roughly 45° and reduces the average moment along the bend direction (figure 6). Furthermore, it is found that the torsion of the ester plane connecting the central ring with both legs deviates markedly from chlorine substituted banana-shaped molecules which have the opposite direction of orientation of the carboxylate groups [14].

The anisotropic shifts of equivalent methylene groups in the short chain homologues differ in the two legs, even for the $-CH_3$ groups. The conformations are rigid enough to preserve the different geometries of the two A rings along the chain.

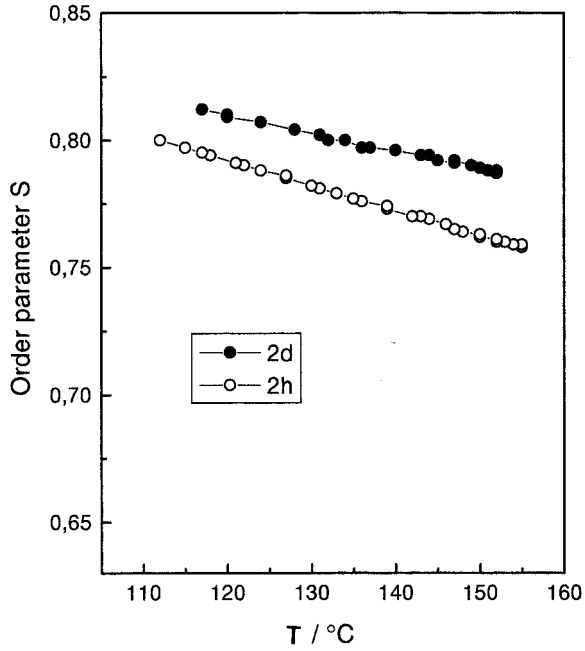

Figure 5. Order parameter $S(T)$ of the B_2 phase of compounds **2d** and **2h** calculated from the anisotropic shifts of carbons in the central ring C (C9H, C9Br, C10H, C10Br).

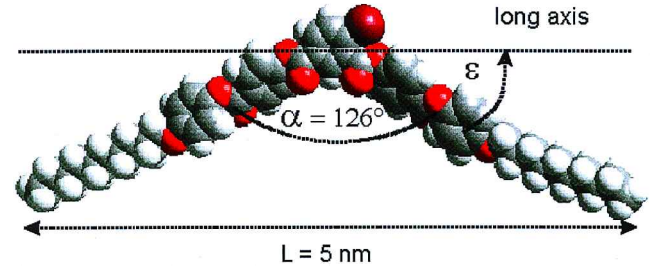

Figure 6. Molecular model of compound **2h** created with Cerius 2.

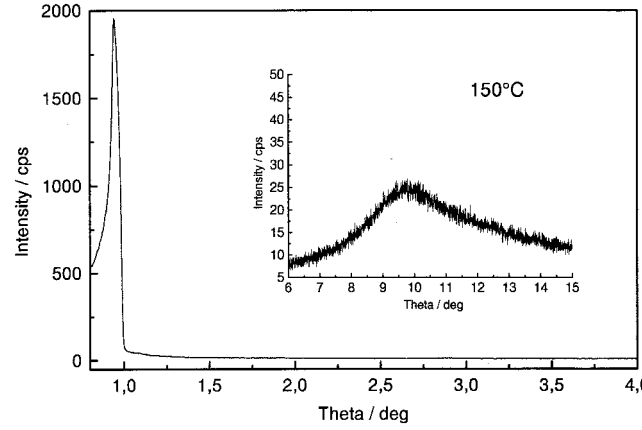

Figure 7. X-ray diffraction pattern of a non-oriented sample of the B_2 phase of compound **2h** (150°C) obtained with Guinier equipment.

Table 3. Geometry of molecular segments in the branches of compounds **1** (H) and compounds **2** (Br); all angles are given in degrees.

	Geometry	Ring A_H	Ring A_{Br}	Ring B_H	Ring B_{Br}	$COO_{Br/H}$
2d	Tilt ε	28.5	30.5	26	27	30[a]
	Torsion φ	44	42.5	44	57	41/37
2h	Tilt ε	29	31	26.5	28	30[a]
	Torsion φ	44	42.5	43	56	45/40

[a] Presumed for a regular aromatic ring.

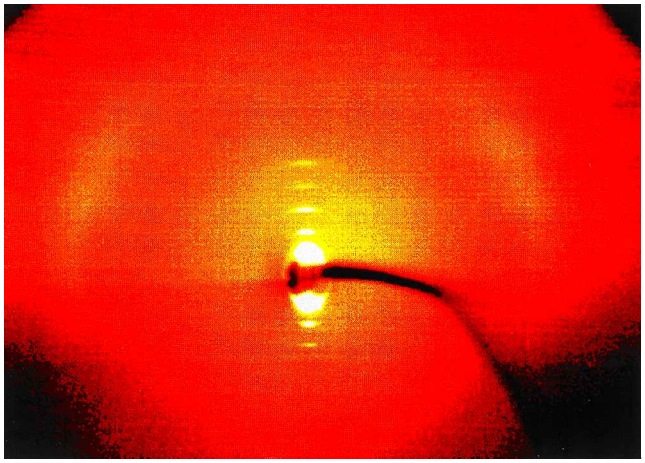

Figure 8. X-ray pattern of a B_2 monodomain of compound **2h** (130°C) recorded with a Siemens HI-Star two-dimensional detector. The orientation was obtained by prolonged annealing of a small drop of the compound on glass surfaces.

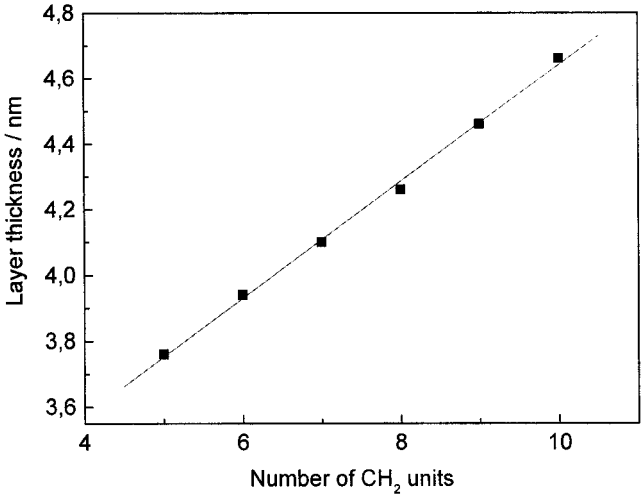

Figure 9. Layer spacings in the B_2 phase as a function of the chain length (compounds **2c**–**2h**) determined with the Guinier equipment.

4.3. *X-ray investigations*

Six compounds (**2c**–**2h**) have been investigated by X-ray diffraction. In figure 7, the X-ray pattern of a non-oriented sample of the mesophase of compound **2h** is

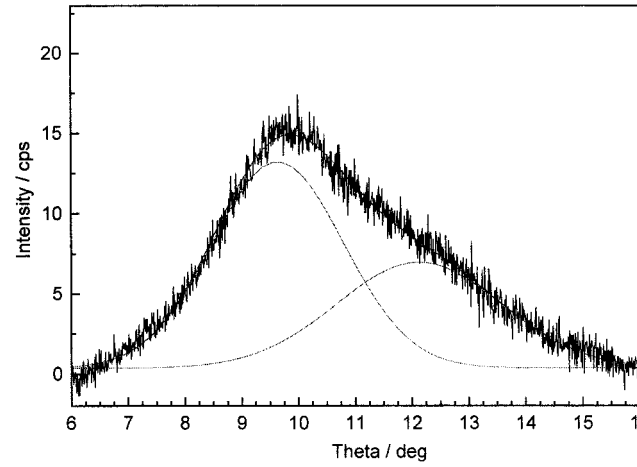

Figure 10. Detailed analysis of the wide angle X-ray scattering of the B_2 phase of compound **2c**. The scattering profile has been fitted by two Gaussian functions. The two maxima correspond to the following lattice distances: $d_1 = 0.45$ nm, $d_2 = 0.36$ nm.

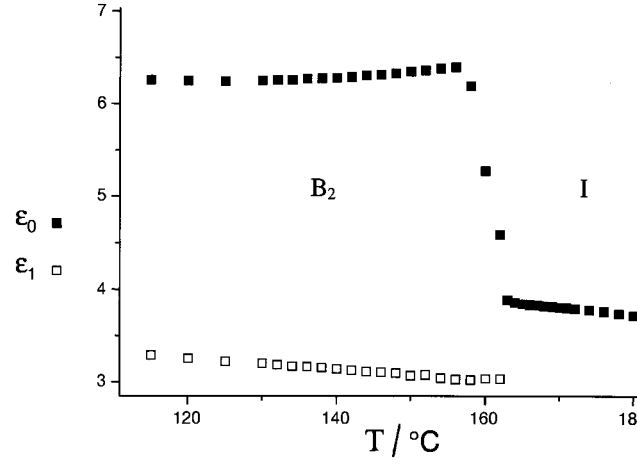

Figure 11. Static (ε_0) and quasi-static (ε_1) dielectric constants of compound **2h** at different temperatures.

presented as a representative example. The pattern of a well oriented monodomain is shown in figure 8. In the small angle region, a strong Bragg reflection and its higher order reflections can be seen, indicating a smectic layer structure. A layer spacing $d = 4.66$ nm could be

determined. For comparison, the length of the bent molecule is about 5 nm using the bending angle of 126° obtained by NMR measurements. The wide angle scattering (~10°) located out of the equator of the pattern is diffuse, which points to a liquid-like order within the smectic layers. From the position of the wide angle scattering maxima with respect to the layer reflections, a tilt angle of 23° can be determined. This means that the bent molecules are tilted with respect to the layer normal which is characteristic of a B_2 phase. Figure 9 displays the layer spacings d in the mesophases of six homologues (**2c**–**2h**). The linear dependence of the d-values on the chain length indicates that the aliphatic chains take a more or less all-*trans*-conformation.

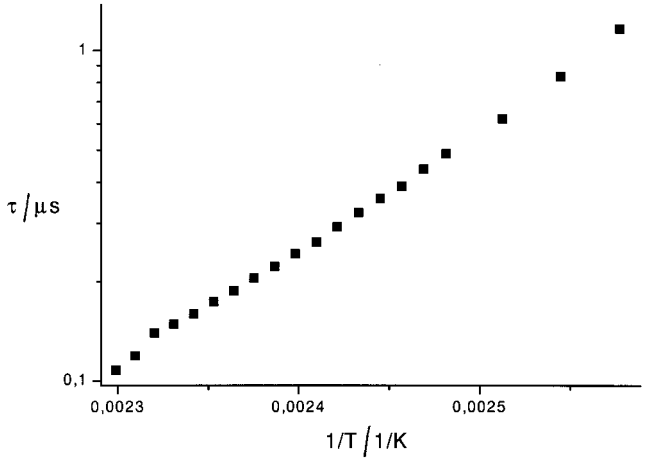

Figure 12. Relaxation times τ as a function of the reciprocal absolute temperature of compound **2h**.

The Guinier-film patterns of the short chain homologues in particular suggest a second diffuse scattering maximum in the wide angle region. In the case of the long chain compounds, the outer diffuse scattering is more smeared out, so that the two maxima can hardly be separated. This can be explained by the lower proportion of Br relative to the whole molecule. The more detailed analysis of the scattering diagram is shown in figure 10. The scattering curve shown has been obtained by subtracting the background scattering. After this procedure the asymmetric profiles have been fitted by two Gaussian functions. The positions of the maxima yield averaged distances of $d_1 = 0.45$ nm and $d_2 = 0.36$ nm. The first can be attributed to the disordered chains, whereas the second may relate to the Br–Br distances [18]. This is supported by the fact that the unsubstituted (Br free) homologues do not give rise to such scattering. It should be mentioned that the same distance is also found in discotic systems in which it represents the averaged phenyl–phenyl distance in the columns. Therefore, a preferred lateral phenyl–phenyl distance can contribute to the same maximum.

4.4. *Dielectric measurements*

The measurements were carried out on compound **2h** in the frequency range 1 Hz to 10 MHz. The measured dielectric constants and losses were fitted to the Cole–Cole equation [19]. In figure 11, the limiting static (ε_0) and quasi-static dielectric constants (ε_1) and their dependence on temperature are presented for the B_2 phase. Dielectric increments of 2.54 (160°C) and 3.15 (140°C) with a maximum value of 3.36 (156°C) were

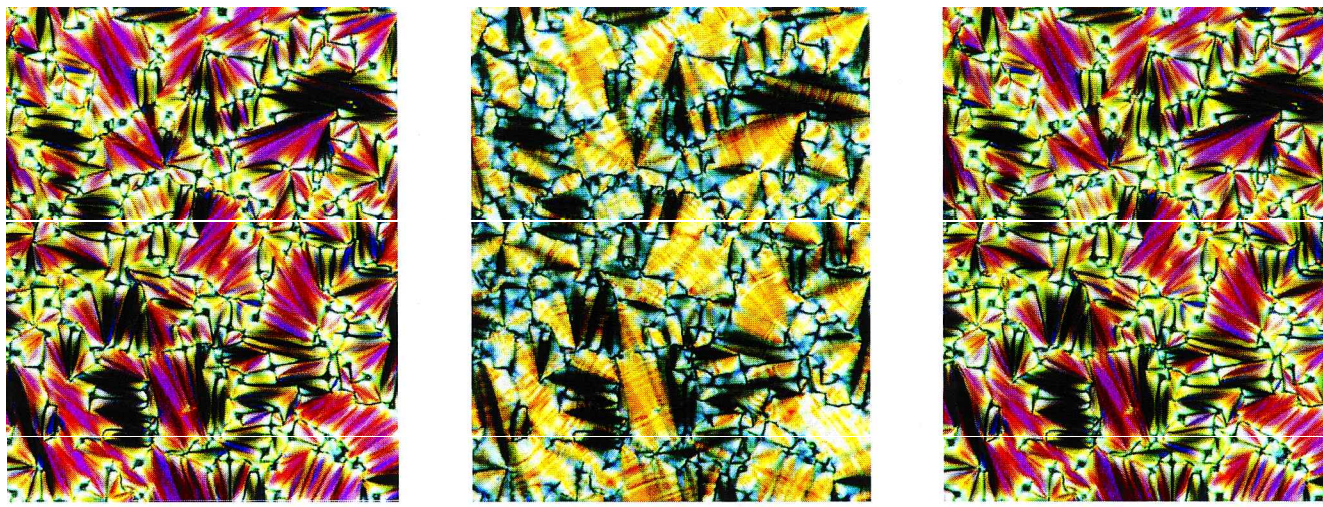

(a) (b) (c)

Figure 13. Dependence of the optical texture on the polarity of the applied electric field: compound **2h**, 4 μm thick EHC cell, 150°C, (*a*) + 30 V, (*b*) 0 V, (*c*) − 30 V.

calculated. The Cole–Cole distribution parameter was estimated to be 0.10. The related relaxation times are shown in figure 12. This high frequency absorption is related to the reorientation of the dipoles around the long axes in the stiff middle parts of the molecules [20].

In the isotropic phase no dielectric absorption could be separated. The dielectric constants of about 3.6 indicate that there must be an additional relaxation process with shorter relaxation times which is out of our experimental range. Measurements on other samples prove the existence of this relaxation range and a stepwise decrease of the relaxation time at the B_2/I transition [20]. The step of one decade is the reason why no absorption in the isotropic phase is seen. The relatively high ε_0 value of the mesophase in comparison with that of the isotropic liquid points to a ferroelectric order in the short range.

The measured dielectric behaviour is, to our knowledge, characteristic for the B_2 phase.

4.5. *Electro-optical investigations*

If an electric field is applied to a 4 μm thick EHC cell, domains with decreasing double refraction grow parallel to the smectic layers giving rise to a red–violet coloured texture (figure 13). As shown in figure 14, this field-induced reorientation is characterized by a domain wall motion which is extended over a limited voltage interval. The textures of the switched states are independent of the polarity of the applied field. Furthermore, the extinction direction does not change on switching. As shown in figure 15 two current peaks could be measured per half period of a triangular voltage waveform indicating an antiferroelectric switching behaviour.

It follows from the model of Link *et al.* [2] that in the homochiral ground state the extinction direction rotates in the opposite direction in relation to the sign of the electric field. In our case, not only are the switched states identical for different signs of the field, but also the extinction direction remains unchanged. This finding is compatible with a racemic antiferroelectric ground state where the tilt of the molecules in successive layers is synclinic and the polar direction alternates [2, 21–23].

5. Concluding remarks

We have prepared several five-ring banana-shaped mesogens derived from isophthalic acid, which are distinguished by the linkage between the aromatic rings and the substitution in the 4-position of the central ring. It was found that the melting and clearing temperatures of the Br-substituted compounds are clearly lower than those of the analogous unsubstituted compounds. In contrast to the Br-substituted compounds, most of the unsubstituted compounds form only a metastable

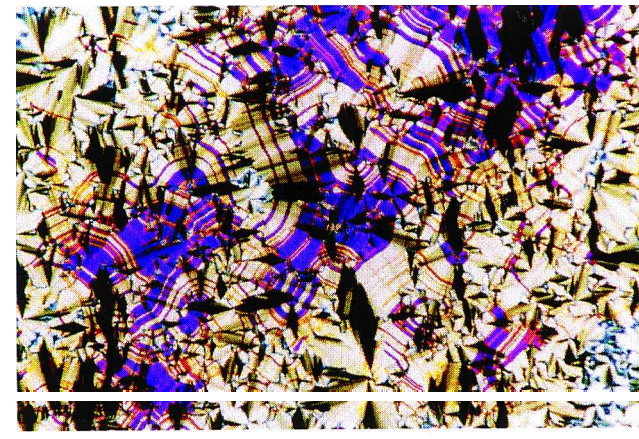

(a)

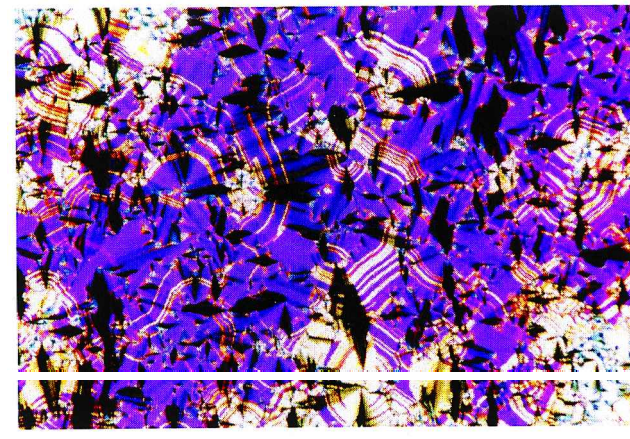

(b)

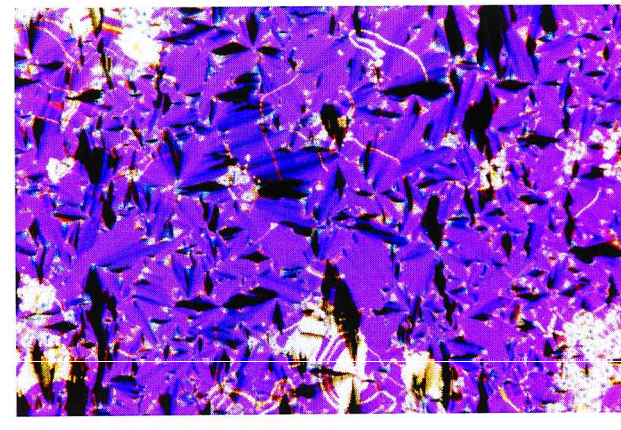

(c)

Figure 14. Dependence of the optical texture on the polarity of the applied electric field: documentation of domain wall motion, compound **2g**, 4 μm thick EHC cell, 147°C; (*a*) + 37 V, (*b*) + 39 V, (*c*) + 41 V.

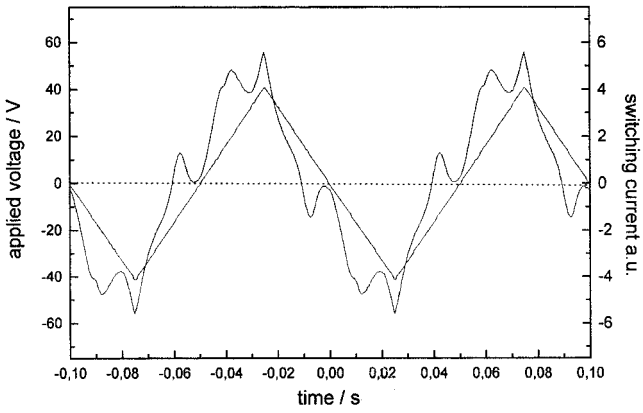

Figure 15. Switching current response in the B_2 phase of compound **2h** on applying a triangular voltage (82.5 V_{pp}, 10 Hz, 160°C).

mesophase. From X-ray diffraction measurements, and dielectric and electro-optical investigations, the mesophase was identified as a B_2 phase. From ^{13}C NMR measurements, it follows that the molecules in the B_2 phase have a bent-shape; for example compounds **2d** and **2h** have an average bending angle of 126°. Furthermore the torsion of the ester plane at the central ring deviates markedly from that in chlorine-substituted compounds which have the opposite direction of orientation of the COO group. The orientational order parameter of the B_2 phase shows a stronger temperature dependence compared with the B_2 phases of other compounds.

References

[1] Niori, T., Sekine, T., Watanabe, J., Furukawa, T., and Takezoe, H., 1996, *J. mater. Chem.*, **6,** 1231.
[2] Link, D. R., Natale, G., Shao, R., Maclennan, J. E., Clark, N. A., Körblova, E., and Walba, D. M., 1997, *Science*, **278,** 1924.
[3] Pelzl, G., Diele, S., and Weissflog, W., 1999, *Adv. Mater.*, **11,** 707.
[4] Shen, D., Diele, S., Pelzl, G., Wirth, I., and Tschierske, C., 1999, *J. mater. Chem.*, **9,** 661.
[5] Sekine, T., Niori, T., Sone, M., Watanabe, J., Choi, S.-W., Takanishi, Y., and Takezoe, H., 1997, *Jpn. J. appl. Phys.*, **36,** 6455.
[6] Weissflog, W., Lischka, Ch., Benne, I., Scharf, T., Pelzl, G., Diele, S., and Kruth, H., 1998, *Proc. SPIE*, **3319,** 14.
[7] Nguyen, H. T., Rouillon, J. C., Marcerou, J. P., Bedel, J. P., Barois, P., and Sarmento, S., 1999, *Mol. Cryst. liq. Cryst.*, **328,** 177.
[8] Heppke, G., Parghi, D. D., and Sawade, H., 2000, *Ferroelectrics*, **243,** 269.
[9] Lee, C. K., and Chien, L. C., 2000, *Ferroelectrics*, **243,** 231.
[10] Sadashiva, B. K., 1999, *Pramana*, **53,** 213.
[11] Diele, S., Grande, S., Kruth, H., Lischka, Ch., Pelzl, G., Weissflog, W., and Wirth, I., 1998, *Ferroelectrics*, **212,** 169.
[12] Pelzl, G., Diele, S., Jakli, A., Lischka, Ch., Wirth, I., and Weissflog, W., 1999, *Liq. Cryst.*, **26,** 135.
[13] Weissflog, W., Lischka, Ch., Diele, S., Pelzl, G., and Wirth, I., 1999, *Mol. Cryst. liq. Cryst.*, **328,** 101.
[14] Pelzl, G., Diele, S. Grande, S., Jakli, A., Lischka, Ch., Kresse, H., Schmalfuss, H., Wirth, I., and Weissflog, W., 1999, *Liq. Cryst.*, **26,** 401.
[15] Weissflog, W., Kovalenko, L., Wirth, I., Diele, S., Pelzl, G., Schmalfuss, H., and Kresse, H., 2000, *Liq. Cryst.*, **27,** 677.
[16] Weissflog, W., Lischka, Ch., Diele, S., Pelzl, G., Wirth, I., Grande, S., Kresse, H., Schmalfuss, H., Hartung, H., and Stettler, A., 1999, *Mol. Cryst. liq. Cryst.*, **333,** 203.
[17] Dehne, H., Pötter, M., Sokolowski, S., Holzlehner, U., Reinke, H., Weissflog, W., Diele, S., Pelzl, G., Wirth, I., Kresse, H., Schmalfuss, H., and Grande, S., 2000, in Proceedings of the Freiburger Arbeitstagung Flüssigkristalle, 2000, P 23.
[18] Bondi, A., 1964, *J. phys. Chem.*, **68,** 441.
[19] Hill, E., Vaughan, W. E., Price, A. H., and Davies, M., 1969, *Dielectric Properties and Molecular Behaviour* (London: van Nostrand, Reinhold), p. 49.
[20] Schmalfuss, H., Shen, D., Tschierske, C., and Kresse, H., 1999, *Liq. Cryst.*, **26,** 1767.
[21] Jakli, A., Lischka, Ch., Weissflog, W., Rauch, S., and Heppke, G., 1999, *Mol. Cryst. liq. Cryst.*, **328,** 299.
[22] Heppke, G., Jakli, A., Rauch, S., and Sawade, H., 1999, *Phys. Rev. E.*, **60,** 5575.
[23] Zennyoji, M., Takanishi, Y., Ishikawa, K., Thisayukta, J., Watanabe, J., and Takezoe, H., 1999, *J. mat. Chem.*, **9,** 2775.